



Since January 2020 Elsevier has created a COVID-19 resource centre with free information in English and Mandarin on the novel coronavirus COVID-19. The COVID-19 resource centre is hosted on Elsevier Connect, the company's public news and information website.

Elsevier hereby grants permission to make all its COVID-19-related research that is available on the COVID-19 resource centre - including this research content - immediately available in PubMed Central and other publicly funded repositories, such as the WHO COVID database with rights for unrestricted research re-use and analyses in any form or by any means with acknowledgement of the original source. These permissions are granted for free by Elsevier for as long as the COVID-19 resource centre remains active.



## Research paper

## Dual inhibition of SARS-CoV-2 and human rhinovirus with protease inhibitors in clinical development

Cheng Liu<sup>a,1</sup>, Sandro Boland<sup>b,1</sup>, Michael D. Scholle<sup>c,1</sup>, Dorothee Bardiot<sup>b</sup>, Arnaud Marchand<sup>b</sup>, Patrick Chaltin<sup>b,e</sup>, Lawrence M. Blatt<sup>a</sup>, Leonid Beigelman<sup>a</sup>, Julian A. Symons<sup>a</sup>, Pierre Raboisson<sup>d</sup>, Zachary A. Gurard-Levin<sup>c</sup>, Koen Vanduyck<sup>d</sup>, Jerome Deval<sup>a,\*</sup>

<sup>a</sup> Aligos Therapeutics, Inc., South San Francisco, USA

<sup>b</sup> Cistim, Leuven, Belgium

<sup>c</sup> SAMDI Tech, Inc., Chicago, USA

<sup>d</sup> Aligos Belgium BV, Leuven, Belgium

<sup>e</sup> Centre for Drug Design and Discovery (CD3), KU Leuven, Leuven, Belgium



## ARTICLE INFO

## Keywords:

COVID-19

Coronavirus

3CLpro

Rhinovirus

Protease inhibitor

Mass spectrometry

## ABSTRACT

The 3-chymotrypsin-like cysteine protease (3CLpro) of severe acute respiratory syndrome coronavirus 2 (SARS-CoV-2) is considered a major target for the discovery of direct antiviral agents. We previously reported the evaluation of SARS-CoV-2 3CLpro inhibitors in a novel self-assembled monolayer desorption ionization mass spectrometry (SAMDI-MS) enzymatic assay (Gurard-Levin et al., 2020). The assay was further improved by adding the rhinovirus HRV3C protease to the same well as the SARS-CoV-2 3CLpro enzyme. High substrate specificity for each enzyme allowed the proteases to be combined in a single assay reaction without interfering with their individual activities. This novel duplex assay was used to profile a diverse set of reference protease inhibitors. The protease inhibitors were grouped into three categories based on their relative potency against 3CLpro and HRV3C including those that are: equipotent against 3CLpro and HRV3C (GC376 and calpain inhibitor II), selective for 3CLpro (PF-00835231, calpain inhibitor XII, boceprevir), and selective for HRV3C (rupintrivir). Structural analysis showed that the combination of minimal interactions, conformational flexibility, and limited bulk allows GC376 and calpain inhibitor II to potently inhibit both enzymes. In contrast, bulkier compounds interacting more tightly with pockets P2, P3, and P4 due to optimization for a specific target display a more selective inhibition profile. Consistently, the most selective viral protease inhibitors were relatively weak inhibitors of human cathepsin L. Taken together, these results can guide the design of cysteine protease inhibitors that are either virus-specific or retain a broad antiviral spectrum against coronaviruses and rhinoviruses.

### 1. Introduction

COVID-19, a respiratory infection caused by severe acute respiratory syndrome coronavirus 2 (SARS-CoV-2), was first detected in China in December 2019 before becoming a global pandemic in 2020. Although >80% of infected individuals are either completely asymptomatic or experience self-limiting symptoms similar to the common cold, clinical cases of severe COVID-19 require hospitalization and intensive care due to pneumonia and extra-pulmonary manifestations (mainly kidney failure, thrombosis, severe inflammation, and central nervous system symptoms) (Harapan et al., 2020). The anti-inflammatory corticosteroid

dexamethasone, and coronavirus (CoV) nucleoside polymerase inhibitor, remdesivir, are considered the standards of care for the treatment of severe COVID-19 in hospitalized patients requiring oxygen or ventilation (<https://www.covid19treatmentguidelines.nih.gov/therapeutic-management/>). However, these molecules are not suitable for early stage SARS-CoV-2 infection, patients with moderate symptoms in hospitalized and outpatient settings, or as prophylaxis. Therefore, the need for additional treatment options adapted to different levels of COVID-19 disease severity remains high.

SARS-CoV-2 is an enveloped, positive-sense, single-stranded RNA virus that belongs to the  $\beta$ -coronavirus genus of the *Coronaviridae* family,

\* Corresponding author.

E-mail address: [jdeval@aligos.com](mailto:jdeval@aligos.com) (J. Deval).

<sup>1</sup> Contributed equally to this work.

which also includes SARS and MERS  $\beta$ -coronaviruses (Coronaviridae Study Group of the International Committee on Taxonomy of 2020). Viral RNA synthesis and processing are controlled by the nonstructural proteins nonstructural protein 7 to 16 after cleavage by the viral 3CL protease (3CLpro) of two large replicase polyproteins translated from the coronavirus genome. The main viral protease, 3CLpro, is a cysteine protease with LQ/(S, A, G) as the preferred P2–P1–P1' substrate sequence (Fan et al., 2005). In comparison, the optimum substrate recognition motif for rhinovirus 3C protease is ETLGQ/GP (Cordingley et al., 1990), highlighting the broad range in substrate recognition among cysteine proteases (Corvo et al., 2018). Due to its key role in viral replication, 3CLpro is considered a major target for antiviral drug discovery. Currently, at least two 3CLpro inhibitors are in (pre)clinical development for the treatment of COVID-19. PF-07304814, is currently in Phase 1 clinical trials in patients with SARS-CoV-2 virus infection and with mild-to-moderate symptoms (NCT04535167). PF-07304814 is a phosphate prodrug with enhanced solubility that is metabolized to the active form PF-00835231 (Boras et al., 2020). In vitro, the inhibitory activity of PF-00835231 is comparable to that of remdesivir against a broad range of coronaviruses (de Vries et al., 2020), with a marked preference for coronavirus proteases over human enzymes (Hoffman et al., 2020). GC376, originally licensed for veterinary use in feline coronavirus infections, is now considered for the treatment of COVID-19 due to its high level of potency against SARS-CoV-2 (Ma et al., 2020). GC376 is a broad-spectrum peptidomimetic agent previously reported to inhibit the replication of noroviruses, picornaviruses, and coronaviruses (Kim et al., 2012; Takahashi et al., 2013; Kim et al., 2016; Pedersen et al., 2018).

Conceptually, developing broad-spectrum antiviral agents targeting coronaviruses and other respiratory viruses such as rhinoviruses is appealing. However, the limited sequence identity between proteases from these two distinct virus families has complicated the design and optimization of dual cysteine protease inhibitors (Wang and Liang 2010). In this study, we evaluated the antiviral spectrum of a set of reference protease inhibitors including PF-00835231 and GC376, as well as calpain inhibitor II and XII, boceprevir, and rupintrivir. We developed a novel duplex biochemical assay optimized to monitor the enzymatic activities of both SARS-CoV-2 3CLpro and rhinovirus HRV3C in the same well. This dual mass spectrometry (MS) readout was used to identify different categories of protease inhibitors based on their relative potency against 3CLpro and HRV3C. Further structural analysis of the active site of both enzymes provides valuable information to guide the design of cysteine protease inhibitors to be either virus specific or retain broad antiviral activity. Our biochemical data also suggest that compounds targeting both coronavirus and rhinovirus proteases are likely to inhibit human cathepsin L. Since cathepsin L is a target for protease inhibitors blocking SARS-CoV-2 cellular entry (Liu et al., 2020; Mellott et al., 2020), the potential implications of these results are discussed.

## 2. Materials and methods

### 2.1. Proteins, peptides, and compounds

SARS-CoV-2 3CLpro was purchased from Kactus and HRV3C was purchased from Sigma (SAE0110). Peptide substrates and internal standards were purchased from BioPeptide (San Diego, CA) at >95% purity. 3CLpro Substrate: Ac-TSAVLQSGFRKK(biotin)-NH<sub>2</sub>, 3CLpro Internal Standard Ac-SAYRKK(biotin)-NH<sub>2</sub>, HRV3C Substrate: Biotin-REEVLFQGGP-NH<sub>2</sub>, HRV3C Internal Standard Biotin-REEVGFQ-NH<sub>2</sub>; Rupintrivir were purchased from Selleck Chemicals (Houston, TX), GC376 was from Biosynth International (Oakbrook Terrace, IL). Calpain inhibitor II was from Sigma Aldrich (St. Louis, MO). Calpain inhibitor XII was from Cayman Chemicals (Ann Arbor, MI). PF-00835231 was prepared as previously outlined (Hoffman et al., 2020). The identity of each compound in DMSO solution was verified by LC-MS (data not shown).

### 2.2. 3CLpro and HRV3C duplex assay

Protease assays were performed in 6  $\mu$ L volume in 384-well low-volume polypropylene microtiter plates (Greiner Bio-One, Kremsmünster, Austria; Catalog 784201) at ambient temperature. The optimized assay buffer was 20 mM Hepes pH 7.5, 10 mM NaCl, 1 mM EDTA, 0.005% bovine skin gelatin (BSG), 0.002% Tween-20, and 1 mM dithiothreitol (DTT). Each enzyme assay was developed individually prior to the duplexing to optimize the buffer, characterize enzyme activity and substrate specificity, determine substrate  $K_M$ , DMSO tolerance, and uniformity. For the duplex assay, 3CLpro (final concentration 3 nM) and HRV3C (final concentration 6 nM) were added using a Multidrop Combi (Thermo Scientific; Waltham, MA) and preincubated for 30 min with test compounds to account for slow on-rates. Reactions were initiated by the addition of the two peptide substrates (final concentration 10  $\mu$ M each). Reactions were incubated for 30 min and quenched by the addition of 0.5% formic acid (final) with subsequent neutralization using 1% sodium bicarbonate (final). Internal standard peptides were added in 20 mM Hepes pH 8.0 (final concentration 100 nM for the 3CLpro internal standard and 750 nM for the HRV3C internal standard) for quantitation of the protease products.

### 2.3. SAMDI-MS analysis

For self-assembled monolayer desorption ionization (SAMDI)-MS analysis, 2  $\mu$ L of each reaction mixture was transferred using a 384-channel automated liquid handler to SAMDI biochip arrays functionalized with a neutravidin-presenting self-assembled monolayer (SAM). The preparation of SAMDI biochip arrays has been previously described (Gurard-Levin et al., 2011). The SAMDI arrays were incubated for 1 h in a humidified chamber to allow the specific immobilization of the biotinylated peptide substrates, cleaved products, and internal standards. The samples were purified by washing the SAMDI arrays with deionized ultrafiltered water (50  $\mu$ L/spot) and dried with compressed air. A matrix comprising alpha-cyano cinnamic acid in 80% acetonitrile:20% aqueous ammonium citrate (10 mg/mL final) was applied in an automated format by dispensing 50 nL to each spot in the array. SAMDI-MS was performed using reflector-positive mode on an AB Sciex TOF-TOF 5800 System (AB Sciex, Framingham, MA) with 400 shots/spot analyzed in a random raster sampling. For data analysis, area under the curve (AUC) peaks for the product and internal standard were calculated using the TOF/TOF Series Explorer (AB Sciex) and the amount of product formed was calculated using the equation (AUC<sub>product</sub>/AUC<sub>internal standard</sub>). Negative controls were pre-quenched with 0.5% formic acid. Assay robustness was determined by Z-Factor, calculated using the equation;

$$1 - (3(\sigma_{\text{pos}} + \sigma_{\text{neg}}) / (\mu_{\text{pos}} - \mu_{\text{neg}}))$$

where  $\sigma$  is the standard deviation and  $\mu$  is the average conversion of the positive and negative control wells.

### 2.4. Human cathepsin L assay

Assays were performed in 20  $\mu$ L volume in 384-well small-volume non-binding microtiter plates (Greiner Bio-One; Monroe, NC) at ambient temperature in the assay buffer (20 mM sodium acetate, 1 mM EDTA, 0.005% Brij-35 and 5 mM DTT pH5.5). Human Cathepsin L (final concentration 10 pM, R&D Systems; Minneapolis, MN) was preincubated for 30 min with test compounds. Reactions were initiated by the addition of a peptide substrate Z-FR-AMC (final concentration 2  $\mu$ M, Anaspec; Fremont, CA). Fluorescence was measured at 2-min intervals for 30 min using a 355/460 excitation/emission filter module on an Envision plate reader (Perkin Elmer; Waltham, MA). The IC<sub>50</sub> values were calculated by fitting the curves using a four-parameter equation in GraphPad Prism.

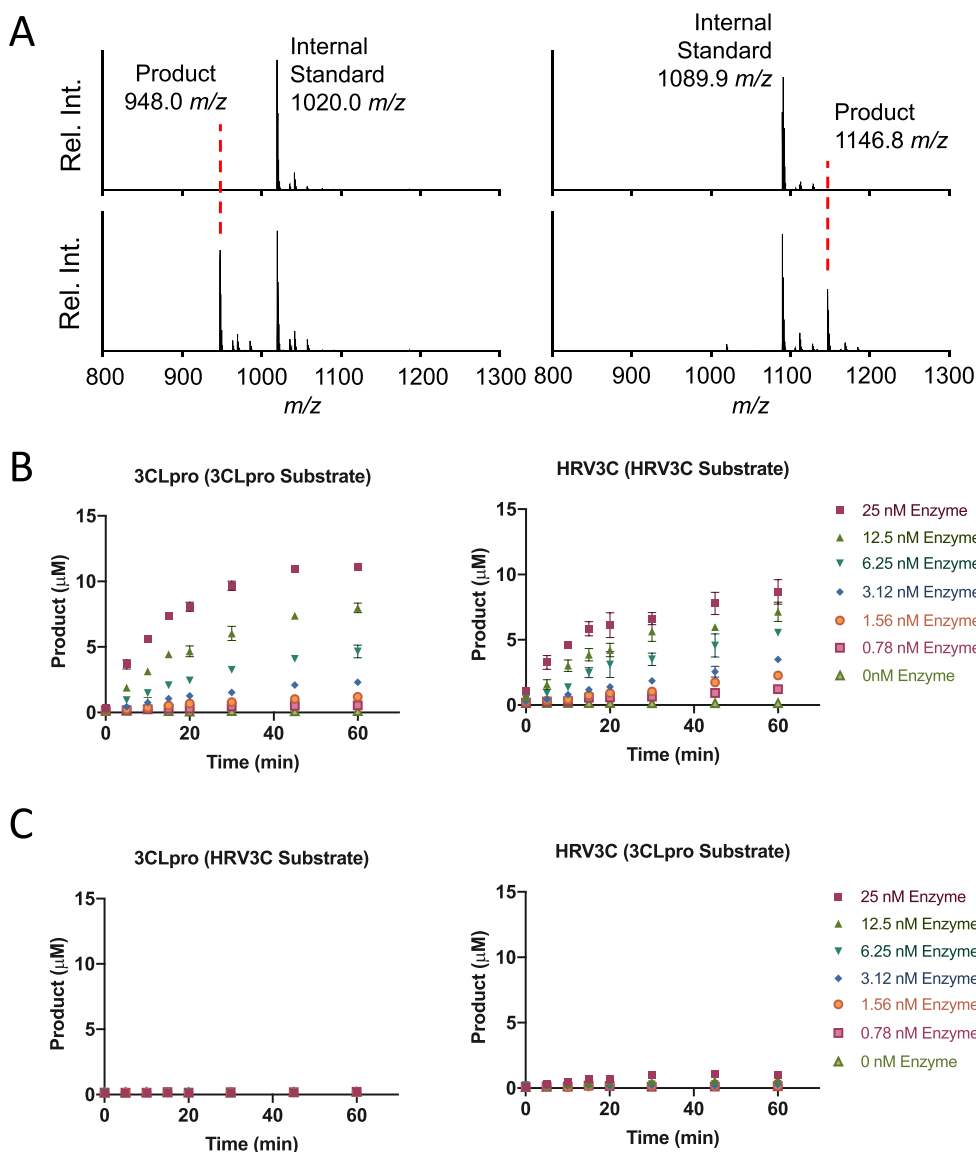


**Fig. 1.** Development of individual 3CLpro and HRV3C SAMDI-MS assays. (A) Representative SAMDI-MS spectra reveal peaks corresponding to internal standards and products from before (top) and after (bottom) 3CLpro (left) and HRV3C (right) activity. (B) The reaction product measured by SAMDI-MS increases with increasing enzyme concentration when matching 3CLpro (left) and HRV3C (right) with their cognate substrates. (C) The lack of product measured by SAMDI-MS when 3CLpro incubates with the HRV3C substrate (left) and HRV3C incubates with the 3CLpro substrate demonstrating enzyme selectivity. All measurements from triplicate data.

## 2.5. Structural analysis

Protein structures for SARS-CoV-2 3CLpro and HRV3C protease were directly retrieved from the Protein Data Bank (PDB) (Berman et al., 2000). PDB identifiers were used for discussion, as some of the structures had yet to be associated with a literature reference at the time of writing this report. Similar structures (e.g. groups of 3CLpro structures or HRV protease structures) were loaded directly into Pymol (The PyMOL Molecular Graphics System, Version 2.0 Schrödinger, LLC.) and superimposed using the default tools. For structures with low identity rates (e.g. 3CLpro vs. HRV protease), PDB structures were first loaded into program Yasara (Krieger and Vriend 2014) and superimposed with SHEBA (Jung and Lee 2000). The transformed coordinates were then saved in PDB format and loaded into Pymol. All subsequent molecular graphics, including protein cartoons and surfaces, were drawn with Pymol.

## 3. Results

### 3.1. Development of a 3CLpro and HRV3C duplex assay

To enable a duplex readout of multiple enzyme activities using

SAMDI-MS, the enzyme product masses must be mass resolvable. Therefore, peptide substrates were designed for 3CLpro and HRV3C to include their respective canonical cleavage sites so that the anticipated cleavage products would be peptides with distinct masses. Each peptide also features a biotin moiety that enables the specific immobilization of the peptide to neutravidin-presenting SAMs following a homogenous reaction in a 384-well plate for MS analysis (Gurard-Levin, 2020). To determine the product masses, 3CLpro and HRV3C were incubated with their cognate substrates in separate reactions and the products analyzed by SAMDI-MS. In the presence of enzyme, the SAMDI-MS spectra for the 3CLpro and HRV3C reactions showed peaks at 948.0  $m/z$  and 1146.8  $m/z$ , respectively, corresponding to each protease product (Supplementary Fig. 1). The distinct masses of the products support their potential application in a duplex SAMDI-MS assay.

To verify selectivity of the two enzymes for their respective substrate, each enzyme was incubated over a range of concentrations of 0.78–25 nM in the presence of each substrate at 10  $\mu\text{M}$  individually and the reactions were monitored over time. Product yields were quantitatively assessed in a SAMDI-MS assay, using internal standard peptides introduced after the reaction. The standards differ from the products in mass but feature similar ionization efficiencies (Gurard-Levin, 2020), enabling a ratiometric analysis to determine yield using the equation

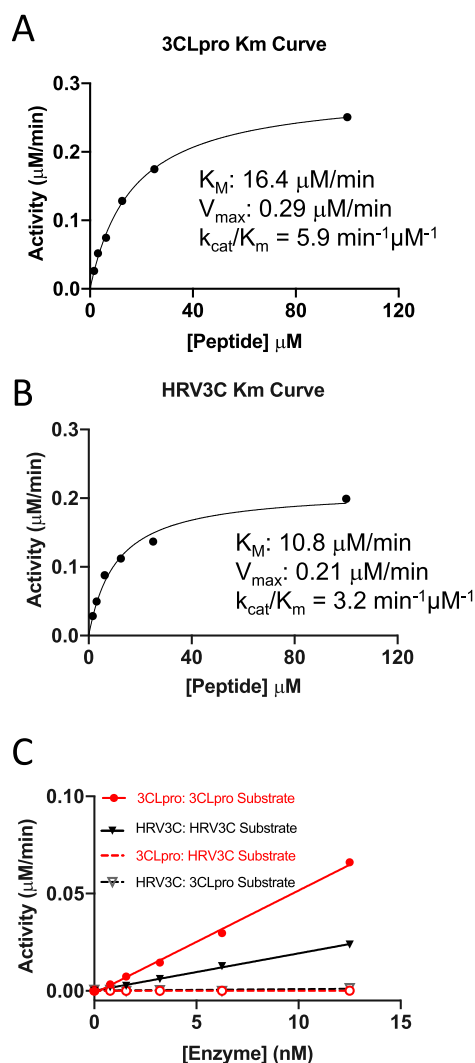


**Fig. 2.** Kinetic parameters for 3CLpro and HRV3C.  $K_M$  and  $V_{max}$  measured for the (A) 3CLpro peptide substrate and (B) HRV3C peptide substrate and respective enzymes. (C) Velocity of 3CLpro and HRV3C activity is linear over a range of concentrations in the SAMDI-MS assay and specific for their peptide substrate (10  $\mu$ M final). All measurements from triplicate data.

$AUC_{prod}/(AUC_{Int\ Std} + AUC_{prod})$  (Fig. 1A). In the presence of their cognate enzyme, product formation accumulated with increasing enzyme concentration (Fig. 1B). Importantly, the HRV3C substrate is not active towards the 3CLpro enzyme, and the 3CLpro substrate exhibits only minimal activity toward HRV3C at 25 nM (Fig. 1C). Below 25 nM, the HRV3C enzyme specifically cleaves its substrate. The selectivity of each enzyme for its substrate provides further support for their potential application in a duplex SAMDI-MS assay.

### 3.2. Determination of kinetic constants and buffer optimization

Before duplexing, the kinetic parameters of each reaction were characterized individually to ensure optimal assay conditions for characterizing inhibitors. Starting with a buffer recently optimized for the 3CLpro protease (Gurard-Levin, 2020), the  $K_M$  and maximum velocity ( $V_{max}$ ) of each peptide substrate was measured in parallel using SAMDI-MS. Concentrations of the two peptides were titrated between 1.5 and 200  $\mu$ M and the product monitored over time. Plotting the initial velocity of the linear portion versus the substrate concentration revealed Michaelis-Menten curves for the two enzymes. The SAMDI-MS assay measured an apparent  $K_M$  of 16.43  $\mu$ M and a  $V_{max}$  of 0.29  $\mu$ M/min for

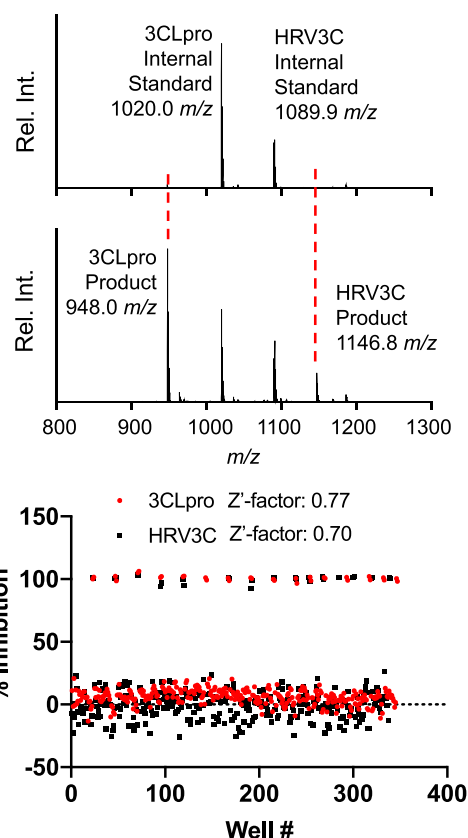


**Fig. 3.** Development of the SAMDI-MS duplexed assay. (A) Representative SAMDI-MS spectra of the duplexed reactions before (top) and after (bottom) 3CLpro and HRV3C activity. (B) Full plate uniformity data using optimized conditions and 6  $\mu$ L reaction volumes for the duplexed SAMDI-MS assay. 100% inhibition controls were pre-incubated with 0.5% formic acid (final).

3CLpro and a  $K_M$  of 10.76  $\mu$ M and  $V_{max}$  of 0.21  $\mu$ M/min for HRV3C, resulting in a  $k_{cat}/K_M$  of 5.9  $\text{min}^{-1}\mu\text{M}^{-1}$  for 3CLpro and 3.2  $\text{min}^{-1}\mu\text{M}^{-1}$  for HRV3C (Fig. 2A and B, Supplementary Fig. 2A). For both enzymes, 10  $\mu$ M peptide was selected to allow for the discovery and characterization of substrate-competitive inhibitors while also ensuring suitable conversion of substrate to product for each enzyme. Using these conditions, activity of each enzyme was measured by SAMDI-MS over a range of enzyme concentrations and the data revealed linear activity up to 12.5 nM of each enzyme (Fig. 2C, Supplementary Fig. 2B). Finally, the impact of glycerol and DMSO was evaluated. The data show that neither glycerol nor DMSO up to 10% significantly impact enzyme activity (Supplementary Fig. 2C), supporting the assay conditions for evaluating small molecule inhibitors dissolved in DMSO. Assay development data converged on the optimal conditions of 10  $\mu$ M of each substrate in the optimized buffer of 20 mM HEPES pH 7.5, 10 mM NaCl, 1 mM EDTA, 0.005% BSG, 0.002% Tween-20, and 1 mM DTT. Under these conditions, 3 nM 3CLpro and 6 nM HRV3C generate suitable amounts of product in a 30-min reaction. Importantly, each enzyme also exhibits specificity for its corresponding substrate (Fig. 2C).

### 3.3. Robustness of the duplex assay

The robustness of each enzyme in the duplex assay is critical to quantitatively measure compound potency and selectivity. To assess the robustness of the duplex SAMDI-MS protease assay, reactions were miniaturized to 6  $\mu$ L in a 384-plate format using the optimized conditions with 3 nM 3CLpro and 6 nM HRV3C. The presence of positive and negative controls permitted calculation of a Z-(or Z')-factor (a measure of robustness), which considers the mean and standard deviation of

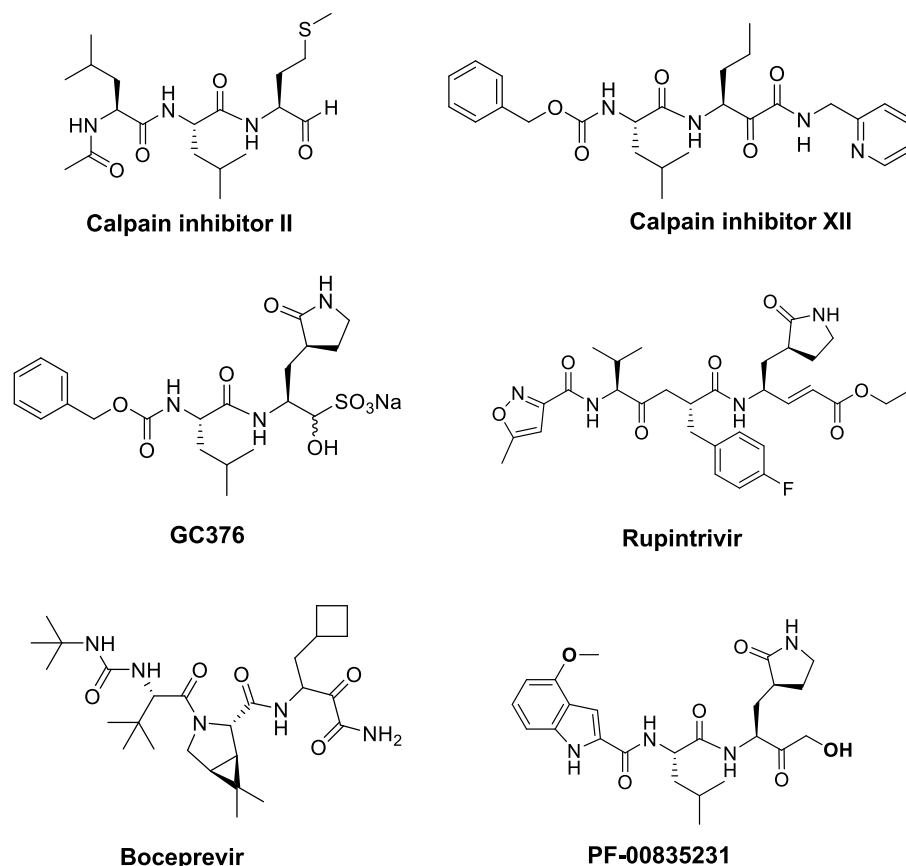


Fig. 4. Structure of reference protease inhibitors used in this study.

positive and negative controls. In this experiment, negative control reactions were pre-quenched with 0.5% formic acid (final concentration). The SAMDI-MS spectra showed peaks corresponding to the two standards and products (Fig. 3A). In a uniformity experiment to measure robustness, the data support a robust assay with  $Z'$ -factors of 0.77 and 0.70 for 3CLpro and HRV3C, respectively (Fig. 3B).

#### 3.4. Evaluation of small molecule inhibitors against viral and human proteases

Next, we evaluated a panel of 3CLpro and HRV3C reported inhibitors in the duplex SAMDI-MS assay (Fig. 4). In the assay, GC376 was equally potent in its inhibition of 3CLpro and HRV3C, with  $IC_{50}$  values of 2.3 and 5.4 nM, respectively (Fig. 5). Likewise, calpain inhibitor II displayed a similar degree of inhibition against the two enzymes. PF-00835231 was about 1000-fold more potent against 3CLpro than HRV3C. Similarly, both calpain inhibitor XII and boceprevir displayed a marked preference for 3CLpro inhibition over HRV3C. In contrast, rupintrivir was selective for HRV3C, with no observed inhibition of 3CLpro. The inhibition potency results obtained in the duplex SAMDI-MS assay were confirmed in the FRET assay format (Supplementary Table 1). In summary, our results distinguish three categories of protease inhibitors based on their relative potency against 3CLpro and HRV3C including those that are: equipotent against 3CLpro and HRV3C (GC376 and calpain inhibitor II), selective for 3CLpro (PF-00835231, calpain inhibitor XII, boceprevir), and selective for HRV3C (rupintrivir).

To evaluate the selectivity of protease inhibitors beyond viral targets, the same six compounds were tested against human cathepsin L. The most potent inhibitors in this assay were GC376 and calpain inhibitor II and XII, with  $IC_{50}$  values below 1 nM (Table 1). PF-00835231 was a moderate inhibitor of human cathepsin L ( $IC_{50}$  ~500 nM). The two commercially approved antiviral protease inhibitors rupintrivir and

boceprevir only weakly inhibited the human enzyme ( $IC_{50} > 1 \mu\text{M}$ ). Taken together, these results indicate that virus-specific protease inhibitors were relatively weak inhibitors of human cathepsin L, whereas molecules with broad antiviral spectrum GC376 and calpain inhibitor II tended to also inhibit the human enzyme.

#### 3.5. Comparison of 3CLpro and HRV3C active sites

GC376, calpain inhibitors II and XII, PF-00835231 and boceprevir have been co-crystallized with 3CLpro, while rupintrivir was not (in line with its lack of activity). However, rupintrivir was co-crystallized with HRV3C protease (PDB 1CQQ & 6KU8), its intended target (Fig. 6A). HRV3C protease and SARS-CoV-2 3C-like protease display a comparable fold, allowing superimposition of the corresponding crystal structures through structural homology methods, e.g., SHEBA (Supplementary Fig. 3). Nonetheless, the identity between the two proteins remains limited (<15%). The primary sequence of HRV3C protease is also notably shorter; missing the C-terminal dimerization domain typical of coronaviral 3C-like proteases. As a result, the proteases differ markedly around positions P2, P3, and P4. The difference is apparent when displaying the molecular surfaces of the proteins around the bound inhibitors, revealing a more open binding site in HRV3C around those positions (Fig. 6A and B). GC376 inhibits 3CLpro by forming a covalent reversible adduct between the catalytic Cys145 and its aldehyde moiety. This functional group represents one of the simplest warheads that can be used to target Cys residues. As a result, GC376 does not display any functional group that could interact—favorably or not—with any of the sub-pockets corresponding to positions P1' and beyond. On the other side of its structure, GC376 is capped by a [(benzyloxy)carbonyl]amino moiety allowing some conformational flexibility. Interestingly, GC376 has been co-crystallized multiple times with SARS-CoV-2 3CLpro (PDB IDs 7C6U, 7CBT, 7C8U, 7BRR, 6WTT, 6WTK, 6WTJ). While the carbonyl

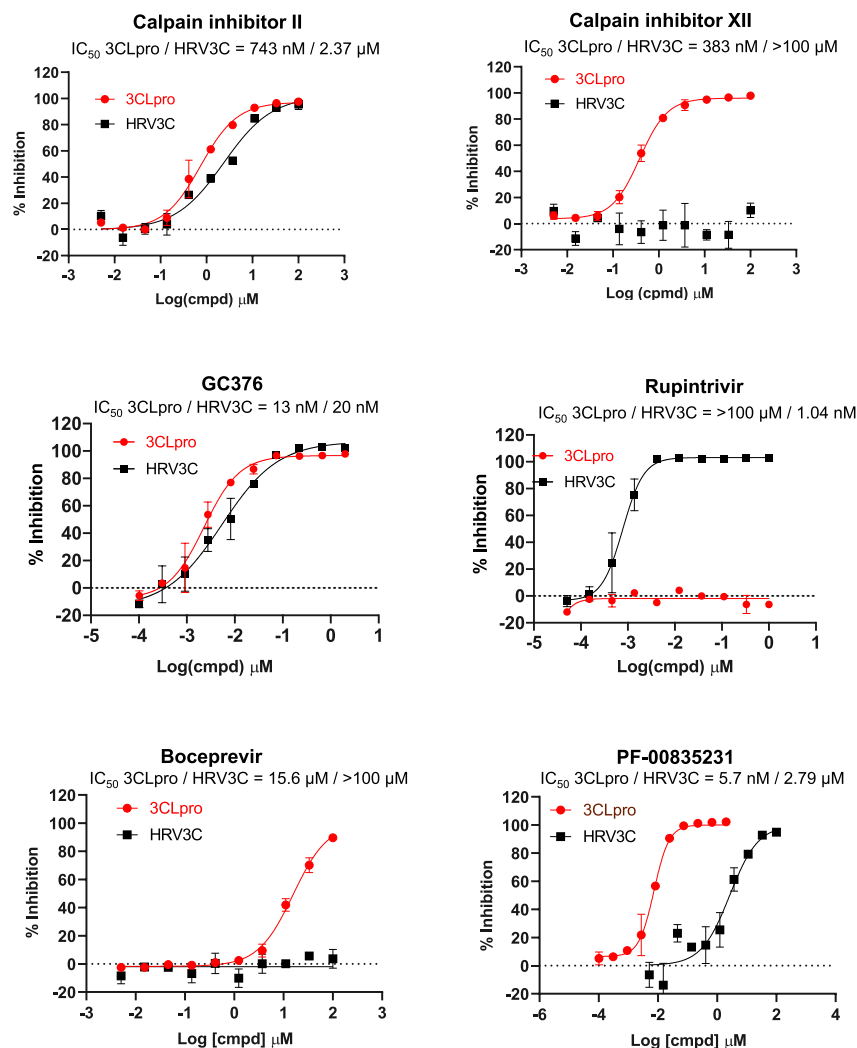


**Fig. 5.** Inhibition of 3CLpro and HRV3C with protease inhibitors.  $IC_{50}$  measurements of 6 reported protease inhibitors measured in the duplexed SAMDI-MS assay against 3CLpro (red) and HRV3C (black). Experiments were performed in duplicate and error bars represent standard deviation.

**Table 1**

Summary of inhibition potency against 3CLpro, HRV3C, and cathepsin L.

Compound	SAMDI-MS 3CLpro $IC_{50}$ (duplex)	SAMDI-MS HRV3C $IC_{50}$ (duplex)	FRET Cathepsin L $IC_{50}$
GC376	13 nM	20 nM	0.33 nM
Boceprevir	15.6 $\mu$ M	>100 $\mu$ M	2.3 $\mu$ M
Calpain inhibitor II	743 nM	2.37 $\mu$ M	0.097 nM
Calpain inhibitor XII	383 nM	>100 $\mu$ M	0.69 nM
Rupintrivir	>100 $\mu$ M	1.04 nM	4.4 $\mu$ M
PF-00835231	5.7 nM	2.79 $\mu$ M	456 nM

of the [(benzyloxy)carbonyl]amino moiety consistently forms an H-bond interaction with the backbone of Glu166 and can therefore be considered a real “anchor point,” the benzyl group adopts multiple conformations, suggesting that only limited interactions are made (Fig. 6C). In the majority of cases, the benzyl group is “folded” toward sub-pocket P3 and the pyrrolidinone moiety occupying sub-pocket P1. The corresponding region (P3) can essentially be considered solvent-exposed in both 3CLpro and HRV3C protease. Similarly, calpain inhibitor II binds 3CLpro through a minimal aldehyde moiety and positions an isobutyl (Leucine) side chain into the P3 region, making only limited contacts. Compared with GC376, calpain inhibitor II forms an additional

H-bond through its acetamide moiety, but lacks the bulky 5-methyl-1,2-oxazol-3-yl moiety found in rupintrivir. In summary, the combination of minimal interactions (essentially with P1 and P2), conformational flexibility, and limited bulk allows GC376 and calpain inhibitor II to inhibit both 3CLpro and HRV3C proteases, despite the low sequence identity between them. In contrast, compounds interacting more tightly with pockets P2, P3, and P4 and/or optimized for a specific target display a more selective inhibition profile.

#### 4. Discussion

This study describes the use of self-assembled monolayer desorption ionization mass spectrometry (SAMDI-MS) technology to develop a novel label-free and duplex biochemical assay containing SARS-CoV-2 3CLpro and rhinovirus HRV3C in the same well. Monitoring the activity of both enzymes simultaneously represents a significant advantage over traditional biochemical assays for routine inhibitor profiling and structure-activity relationship studies. The main change in assay conditions compared to our previous report of the SAMDI-MS readout is the use of tag-free SARS-CoV-2 3CLpro (Gurard-Levin et al., 2020). Using a native construct instead of an MBP-tagged protein resulted in about 100-fold increase in enzymatic activity ( $k_{cat}/K_m = 5.9 \text{ min}^{-1}\mu\text{M}^{-1}$  for native 3CLpro vs.  $0.058 \text{ min}^{-1}\mu\text{M}^{-1}$  for MBP-3CLpro) (Fig. 2A). We evaluated the antiviral spectrum of a set of reference protease inhibitors

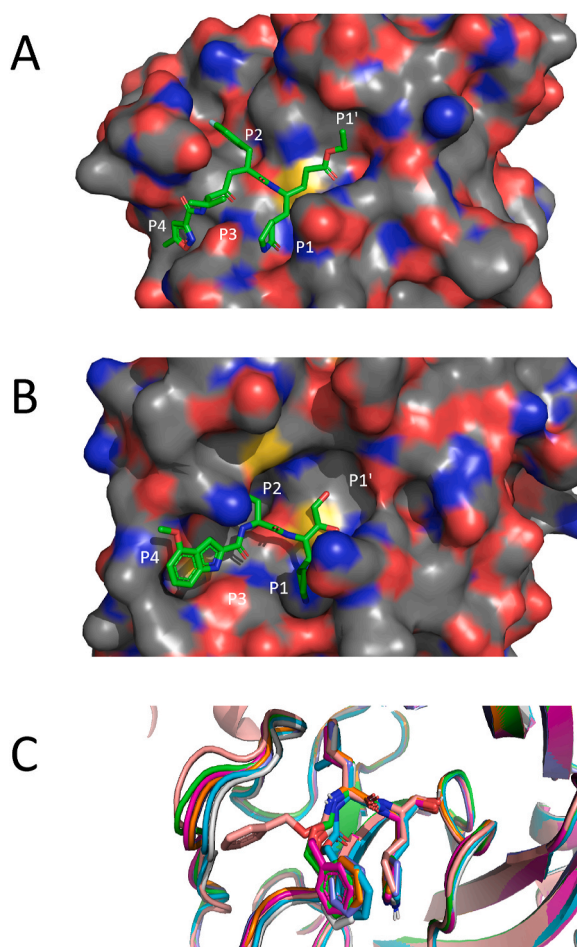


**Fig. 6.** Structural analysis of protease inhibitor binding sites. (A) and (B): Binding mode of rupintrivir in HRV3C protease (A; PDB 1CQQ) and of PF-00835231 in SARS-CoV-2 3C-like protease (B; PDB 6XMH). Proteins were superimposed with SHEBA and drawn as molecular surfaces with Pymol. Inhibitors are displayed as green sticks. (C) Superimposition of reported structures of SARS-CoV-2 3CLpro with bound GC376 (7C6U green, 7CBT cyan, 7C8U magenta, 6WTT tan, 7BRR light grey, 6WTK blue, 6WTJ orange). The terminal benzyl group of GC376 is found in multiple conformations, but is in most cases oriented toward the solvent-exposed sub-pocket P3 and the pyrrolidinone moiety occupying sub-pocket P1. Closer contact with the protein is only suggested for structure 6WTT; wherein the benzyl group is oriented toward P4.

including PF-00835231 and GC376, as well as calpain inhibitor II and XII, boceprevir, and rupintrivir (Fig. 4). There again, changing the enzyme source to the native construct resulted in a 5–10-fold increase of inhibition potency for GC376 as well as calpain inhibitors II and XII (Fig. 5). This increased potency can be explained by the lower enzyme concentration used for the native construct (3 nM) vs. MBP-3CLpro (125 nM). Importantly, our 3CLpro IC<sub>50</sub> values are in good agreement with previous reports for all compounds including the clinical candidate PF-00835231 (Boras et al., 2020; Hoffman et al., 2020; Ma et al., 2020). Our results also reveal that GC376 and PF-00835231, the two most studied protease inhibitors for the treatment of SARS-CoV-2, have very distinct selectivity profiles. GC376 is a very broad cysteine protease inhibitor with no selectivity for 3CLpro over HRV3C and cathepsin L. On the other hand, PF-00835231 inhibits SARS-CoV-2 3CLpro about 100- and 500-fold more potently than cathepsin L and HRV 3C, respectively (Table 1). Since cathepsin L is a target for protease inhibitors blocking SARS-CoV-2 cellular entry, targeting both 3CLpro and cathepsin L with a single molecule could potentially have a synergistic antiviral effect at least in cell culture systems (Liu et al., 2020; Mellott et al., 2020).

However, the antiviral benefit of inhibiting cathepsin L alone or together with 3CLpro in the context of COVID-19 still needs to be demonstrated in animal models and in the clinic.

One of the objectives of our study was to define the molecular bases for the selectivity of cysteine protease inhibitors. When binding HRV3C protease, the selective inhibitor rupintrivir positions a 4-fluorophenyl moiety in a P2 “groove” that is partially exposed, in contrast to the more enclosed sub-pocket found in SARS-CoV-2 3CLpro. Such a 4-fluorophenyl moiety was recently reported to decrease the activity of structurally related compounds against SARS-CoV-2 3CLpro (Zhang et al., 2020). Rupintrivir also binds in an extended conformation that would not be accepted by SARS-CoV-2 3CLpro. In particular, the [(5-methyl-1,2-oxazol-3-yl)formamido] moiety, which makes several favorable contacts in HRV3C protease, would sterically conflict with the amino-acid section connecting the catalytic and dimerization domains of SARS-CoV-2 3CLpro. The other selective inhibitor boceprevir displays a rigid and hydrophobic 3,3-dimethylbutanoyl-6,6-dimethyl-3-azabicyclo[3.1.0]hexan-2-yl moiety, which occupies P2 instead of the more usual leucine residue found in other 3CLpro inhibitors as in consensus substrates. This elaborate group makes multiple hydrophobic contacts with two methionine residues (M49, M165), which are absent from HRV3C protease (one replaced by glycine, one having no corresponding residue; yielding the more open binding site around P2). Both selective inhibitors boceprevir and PF-00835231 form multiple contacts with the amino-acid section connecting the catalytic and dimerization domains of SARS-CoV-2 3CLpro, which is missing from HRV3C protease. Of note, the 4-methoxy-indole group found in PF-00835231 results from a dedicated optimization of the compound series against 3CLpro (Hoffman et al., 2020). The lack of corresponding contacts in HRV3C protease explains the selectivity of this inhibitor toward 3CLpro. On the other hand, the simple warhead of GC376 and its lack of targeted functional groups explain its ability to potentially inhibit not only SARS-CoV-2 3CLpro and HRV3C protease, but also human cathepsin L (Fig. 5 and Table 1).

Can a protease inhibitor potentially target coronaviruses and picornaviruses without inhibiting human proteases? Our structural analyses indicate that compounds optimized to interact tightly with specific pockets of their protein target site tend to display a more selective inhibition profile. Therefore, optimizing a protease inhibitor for broad antiviral spectrum against coronaviruses and picornaviruses without also inhibiting the human counterparts might be challenging, but theoretically achievable. The inhibition of human proteases by clinical stage PF-00835231, boceprevir, and rupintrivir has been described and these compounds are relatively selective (Dragovich et al., 1999; Howe and Venkatraman 2013; Hoffman et al., 2020). This selectivity profile is consistent with our own results showing preferred inhibition for one viral protease (Table 1). Calpain inhibitor XII, while most active on calpain I, is active vs. calpain II and cathepsin B and L (Li et al., 1996; Sacco et al., 2020). Therefore, our observation that calpain inhibitor XII does not inhibit HRV3C does not mean that this compound is a selective protease inhibitor (Table 1). Also calpain inhibitor II is described to inhibit human cysteine proteases calpain I, II, cathepsin L and cathepsin B (Sasaki et al., 1990). Furthermore, while inhibitor GC376 does contain a glutamine surrogate in the P1-position and a consensus leucine on P2, this is not considered sufficient to render selectivity for viral proteases, especially as the released active GC373 is a reactive aldehyde. GC373 is known to inhibit cathepsin B with an IC<sub>50</sub> value of 9 nM (Swisher et al., 2015). These data are consistent with a very recent study showing that GC373 and GC376 inhibit cathepsin L (<https://doi.org/10.1101/2020.11.21.392753>). In summary, our 3CLpro/HRV3C duplex assay provides a convenient way to rapidly and systematically measure the antiviral selectivity of clinically relevant protease inhibitors. Coupled with cathepsin L testing, our analyses indicate that dual inhibition of SARS-CoV-2 and human rhinovirus proteases can be achieved with molecules like GC376 and calpain inhibitor II, but that this broad antiviral spectrum also extends to human proteases such as cathepsin L. The

potential benefit of inhibiting 3CLpro together with cathepsin L for the treatment of COVID-19 will require further investigation.

## Funding

Aligos Therapeutics, Inc. provided funding for this study. The funders had no role in study design, data collection and analysis, decision to publish, or preparation of the manuscript.

## Declaration of competing interest

I have read the journal's policy and the authors of this manuscript have the following competing interests: Cheng Liu, Lawrence M. Blatt, Leonid Beigelman, Julian A. Symons, Pierre Raboisson, Koen Vandyck, and Jerome Deval are current employees of Aligos Therapeutics. Sandro Boland, Dorothee Bardiot, Arnaud Marchand, and Patrick Chaltin are current employees of Cistim/KU Leuven. Michael D. Scholle and Zachary A. Gurard-Levin are current employees of SAMDI Tech.

## Acknowledgements

We thank Peggy Korn for her careful editorial review of the manuscript, and Caroline Williams for LC-MS analysis.

## Appendix A. Supplementary data

Supplementary data to this article can be found online at <https://doi.org/10.1016/j.antiviral.2021.105020>.

## References

- Berman, H.M., Westbrook, J., Feng, Z., Gilliland, G., Bhat, T.N., Weissig, H., Shindyalov, I.N., Bourne, P.E., 2000. The protein Data Bank. *Nucleic Acids Res.* 28 (1), 235–242.
- Boras, B., Jones, R.M., Anson, B.J., Arenson, D., Aschenbrenner, L., Bakowski, M.A., Beutler, N., Binder, J., Chen, E., Eng, H., Hammond, J., Hoffman, R., Kadar, E.P., Kania, R., Kimoto, E., Kirkpatrick, M.G., Lanyon, L., Lendy, E.K., Lillis, J.R., Luthra, S.A., Ma, C., Noell, S., Obach, R.S., O'Brien, M.N., O'Connor, R., Ogilvie, K., Owen, D., Pettersson, M., Reese, M.R., Rogers, T., Rossulek, M.I., Sathish, J.G., Steppan, C., Ticehurst, M., Updyke, L.W., Zhu, Y., Wang, J., Chatterjee, A.K., Mesecar, A.D., Anderson, A.S., Allerton, C., 2020. Discovery of a Novel Inhibitor of Coronavirus 3CL Protease as a Clinical Candidate for the Potential Treatment of COVID-19. *bioRxiv*.
- Cordingley, M.G., Callahan, P.L., Sardana, V.V., Garsky, V.M., Colonna, R.J., 1990. Substrate requirements of human rhinovirus 3C protease for peptide cleavage in vitro. *J. Biol. Chem.* 265 (16), 9062–9065.
- Coronaviridae Study Group of the International Committee on Taxonomy of V, 2020. The species Severe acute respiratory syndrome-related coronavirus: classifying 2019-nCoV and naming it SARS-CoV-2. *Nat. Microbiol.* 5 (4), 536–544.
- Corvo, I., Ferraro, F., Merlino, A., Zuberbuhler, K., O'Donoghue, A.J., Pastro, L., Pidenis, N., Basika, T., Roche, L., McKerrow, J.H., Craik, C.S., Caffrey, C.R., Tort, J.F., 2018. Substrate specificity of cysteine proteases beyond the S2 pocket: mutagenesis and molecular dynamics investigation of fasciola hepatica cathepsins L. *Front. Mol. Biosci.* 5, 40.
- de Vries, M., Mohamed, A.S., Prescott, R.A., Valero-Jimenez, A.M., Desvignes, L., O'Connor, R., Steppan, C., Anderson, A.S., Binder, J., Dittmann, M., 2020. Comparative Study of a 3CL (Pro) Inhibitor and Remdesivir against Both Major SARS-CoV-2 Clades in Human Airway Models. *bioRxiv*.
- Dragovich, P.S., Prins, T.J., Zhou, R., Webber, S.E., Marakovits, J.T., Fuhrman, S.A., Patick, A.K., Matthews, D.A., Lee, C.A., Ford, C.E., Burke, B.J., Rejto, P.A., Hendrickson, T.F., Tuntland, T., Brown, E.L., Meador 3rd, J.W., Ferre, R.A., Harr, J. E., Kosa, M.B., Worland, S.T., 1999. Structure-based design, synthesis, and biological evaluation of irreversible human rhinovirus 3C protease inhibitors. 4. Incorporation of P1 lactam moieties as L-glutamine replacements. *J. Med. Chem.* 42 (7), 1213–1224.
- Fan, K., Ma, L., Han, X., Liang, H., Wei, P., Liu, Y., Lai, L., 2005. The substrate specificity of SARS coronavirus 3C-like proteinase. *Biochem. Biophys. Res. Commun.* 329 (3), 934–940.
- Gurard-Levin, Z.A., Liu, C., Jekle, A., Jaisinghani, R., Ren, S., Vandyck, K., Jochmans, D., Leyssen, P., Neyts, J., Blatt, L.M., Beigelman, L., Symons, J.A., Raboisson, P., Scholle, M.D., Deval, J., 2020. Evaluation of SARS-CoV-2 3C-like protease inhibitors using self-assembled monolayer desorption ionization mass spectrometry. *Antivir. Res.* 182, 104924.
- Gurard-Levin, Z.A., Scholle, M.D., Eisenberg, A.H., Mrksich, M., 2011. High-throughput screening of small molecule libraries using SAMDI mass spectrometry. *ACS Comb. Sci.* 13 (4), 347–350.
- Harapan, H., Itoh, N., Yufika, A., Winardi, W., Keam, S., Te, H., Megawati, D., Hayati, Z., Wagner, A.L., Mudatsir, M., 2020. Coronavirus disease 2019 (COVID-19): a literature review. *J. Infect. Public Health* 13 (5), 667–673.
- Hoffman, R.L., Kania, R.S., Brothers, M.A., Davies, J.F., Ferre, R.A., Gajiwala, K.S., He, M., Hogan, R.J., Kozminski, K., Li, L.Y., Lockner, J.W., Lou, J., Marra, M.T., Mitchell Jr., L.J., Murray, B.W., Nieman, J.A., Noell, S., Planken, S.P., Rowe, T., Ryan, K., Smith 3rd, G.J., Solowiej, J.E., Steppan, C.M., Taggart, B., 2020. Discovery of ketone-based covalent inhibitors of coronavirus 3CL proteases for the potential therapeutic treatment of COVID-19. *J. Med. Chem.* <https://doi.org/10.1021/acs.jmedchem.0c01063>. PMID: 33054210.
- Howe, A.Y., Venkatraman, S., 2013. The discovery and development of boceprevir: a novel, first-generation inhibitor of the hepatitis C virus NS3/4A serine protease. *J. Clin. Transl. Hepatol.* 1 (1), 22–32.
- Jung, J., Lee, B., 2000. Protein structure alignment using environmental profiles. *Protein Eng.* 13 (8), 535–543.
- Kim, Y., Liu, H., Galasiti Kankanamalage, A.C., Weerasekera, S., Hua, D.H., Groutas, W. C., Chang, K.O., Pedersen, N.C., 2016. Reversal of the progression of fatal coronavirus infection in cats by a broad-spectrum coronavirus protease inhibitor. *PLoS Pathog.* 12 (3), e1005531.
- Kim, Y., Lovell, S., Tiew, K.C., Mandadapu, S.R., Alliston, K.R., Battaile, K.P., Groutas, W. C., Chang, K.O., 2012. Broad-spectrum antivirals against 3C or 3C-like proteases of picornaviruses, noroviruses, and coronaviruses. *J. Virol.* 86 (21), 11754–11762.
- Krieger, E., Vriend, G., 2014. YASARA View - molecular graphics for all devices - from smartphones to workstations. *Bioinformatics* 30 (20), 2981–2982.
- Li, Z., Ortega-Vilain, A.C., Patil, G.S., Chu, D.L., Foreman, J.E., Eveleth, D.D., Powers, J. C., 1996. Novel peptidyl alpha-keto amide inhibitors of calpains and other cysteine proteases. *J. Med. Chem.* 39 (20), 4089–4098.
- Liu, T., Luo, S., Libby, P., Shi, G.P., 2020. Cathepsin L-selective inhibitors: a potentially promising treatment for COVID-19 patients. *Pharmacol. Ther.* 213, 107587.
- Ma, C., Sacco, M.D., Hurst, B., Townsend, J.A., Hu, Y., Szteto, T., Zhang, X., Tarbet, B., Marty, M.T., Chen, Y., Wang, J., 2020. Boceprevir, GC-376, and Calpain Inhibitors II, XII Inhibit SARS-CoV-2 Viral Replication by Targeting the Viral Main Protease. *bioRxiv*.
- Mellott, D., Tseng, C.T., Drelich, A., Fajtova, P., Chenna, B.C., Kostomiris, D., Hsu, J.C., Zhu, J., Taylor, Z., Tat, V., Katzfuss, A., Li, L., Giardini, M.A., Skinner, D., Hirata, K., Beck, S., Carlin, A.F., Clark, A.E., Berreta, L., Maneval, D., Frueh, F., Hurst, B.L., Wang, H., Kocurek, K.I., Rauschel, F.M., O'Donoghue, A., Siqueira-Neto, J.L., Meek, T.D., McKerrow, J.H., 2020. A Cysteine Protease Inhibitor Blocks SARS-CoV-2 Infection of Human and Monkey Cells. *bioRxiv*.
- Pedersen, N.C., Kim, Y., Liu, H., Galasiti Kankanamalage, A.C., Eckstrand, C., Groutas, W. C., Bannasch, M., Meadows, J.M., Chang, K.O., 2018. Efficacy of a 3C-like protease inhibitor in treating various forms of acquired feline infectious peritonitis. *J. Feline Med. Surg.* 20 (4), 378–392.
- Sacco, M.D., Ma, C., Lagarias, P., Gao, A., Townsend, J.A., Meng, X., Dube, P., Zhang, X., Hu, Y., Kitamura, N., Hurst, B., Tarbet, B., Marty, M.T., Kolocouris, A., Xiang, Y., Chen, Y., Wang, J., 2020. Structure and Inhibition of the SARS-CoV-2 Main Protease Reveals Strategy for Developing Dual Inhibitors against M(pro) and Cathepsin L. *bioRxiv*.
- Sasaki, T., Kishi, M., Saito, M., Tanaka, T., Higuchi, N., Kominami, E., Katunuma, N., Murachi, T., 1990. Inhibitory effect of di- and tripeptidyl aldehydes on calpains and cathepsins. *J. Enzym. Inhib.* 3 (3), 195–201.
- Swisher, L.Z., Prior, A.M., Gunaratna, M.J., Shishido, S., Madiyar, F., Nguyen, T.A., Hua, D.H., Li, J., 2015. Quantitative electrochemical detection of cathepsin B activity in breast cancer cell lysates using carbon nanofiber nanoelectrode arrays toward identification of cancer formation. *Nanomedicine* 11 (7), 1695–1704.
- Takahashi, D., Kim, Y., Lovell, S., Prakash, O., Groutas, W.C., Chang, K.O., 2013. Structural and inhibitor studies of norovirus 3C-like proteases. *Virus Res.* 178 (2), 437–444.
- Wang, H.M., Liang, P.H., 2010. Picornaviral 3C protease inhibitors and the dual 3C protease/coronaviral 3C-like protease inhibitors. *Expert Opin. Ther. Pat.* 20 (1), 59–71.
- Zhang, L., Lin, D., Kusov, Y., Nian, Y., Ma, Q., Wang, J., von Brunn, A., Leyssen, P., Lanko, K., Neyts, J., de Wilde, A., Snijder, E.J., Liu, H., Hilgenfeld, R., 2020. Alpha-ketoamides as broad-spectrum inhibitors of coronavirus and enterovirus replication: structure-based design, synthesis, and activity assessment. *J. Med. Chem.* 63 (9), 4562–4578.